Long-term rapamycin treatment suppresses IL-17-producing gamma delta T cells and blunts neuroinflammation in aging.

Clement Torrent[1], Caterina Gagliardi[1], Nina Fülle[1], Ignazio Antignano[1], Maria Eugenia Bernis[1], Miriam Stork[1], Daniele Bano[1], Melania Capasso*[1,2], Lily Keane*[1, 2, 3]

[1] German Center for Neurodegenerative Diseases (DZNE), Bonn, Germany
[2] Barts Cancer Institute, Queen Mary University of London, London, United Kingdom
[3] University College Cork, Cork, Ireland
* corresponding authors: Melania Capasso, melania.capasso@dzne.de, Lily Keane, lilykeane@ucc.ie

Abstract

Aging is the gradual accumulation of structural and functional changes in an organism over time, including immune remodeling and a progressive increase in basal inflammation, or inflammaging. The mTOR pathway is a central driver of aging-related diseases, such as cancer, chronic inflammation and neurodegeneration; pharmacological inhibition with rapamycin is associated with reduced aged-related morbidity and increased lifespan across species. Nonetheless, concerns remain about the use of rapamycin, a well-established immunosuppressant in transplant medicine, as an anti-aging intervention. Here, we evaluated the impact of prolonged low-dose dietary rapamycin on the aging immune system. Treatment did not significantly alter innate or adaptive immune cell populations, including brain resident microglia; however, it attenuated the age-associated accumulation of IL-17–producing γδ T cells, particularly in the peritoneal cavity. After a peripheral inflammatory LPS challenge, circulating IL-17 levels were significantly reduced and correlated with an attenuation of microglia inflammatory phenotype. These findings suggest that prolonged low-dose rapamycin exposure exerts minor systemic immune changes, while selectively limiting age-related γδ T cell expansion and neuroinflammation associated with systemic inflammation.

Introduction

Aging is a process characterized by the progressive manifestation of hallmarks such as stem cell exhaustion, cellular senescence, chronic inflammation and metabolic dysfunction, leading to the loss of physiological homeostasis and increasing risk of death (1, 2). The mechanistic target of rapamycin (mTOR) complex 1 (mTORC1) pathway fine-tunes a majority of these aging hallmarks (3). Therefore, significant attention has been dedicated to understanding the role of the mTORC1 pathway in aging.

The serine-threonine kinase mTOR is activated by a broad range of stimuli, such as growth factors, cytokines and amino acids (4-6) and, when associated with other proteins to form mTOR complex 1, it integrates catabolic and anabolic signals to balance cell metabolism, survival, growth, proliferation, migration, differentiation and immune response (6). Given its critical role in regulating cell responses,

36 mTORC1 activity is tightly linked with several age-related pathologies, such as neurodegenerative
37 diseases, cancers, diabetes, and chronic inflammation (7).

38 In the past two decades, numerous studies have investigated the potential of mTORC1 inhibitors as
39 treatment for several cancers and as immunosuppressants (8-10). One of these inhibitors is rapamycin,
40 the first TOR inhibitor to be identified (11). Rapamycin or Sirolimus has been widely used in
41 transplantation for its immunosuppressive properties (12). Paradoxically, short-term rapamycin
42 treatment has also been shown to enhance vaccine responses, an effect attributed in part to heightened
43 myeloid cell activity (13-16). Beyond its immunomodulatory roles, renewed interest in rapamycin and
44 mTORC1 inhibition was sparked by the discovery that rapamycin extends lifespan (17, 18), an effect
45 thought to be mediated largely through suppression of cancer development (8). Nonetheless, while
46 accumulating evidence suggests that rapamycin ameliorates certain aspects of age-associated
47 inflammation, its overall impact on the aging immune system remains incompletely understood. Notably,
48 literature remains elusive on how rapamycin modulates acute systemic inflammatory responses in aging,
49 for example responses to systemic LPS. For these reasons, doubts remain on whether long-term *in vivo*
50 rapamycin treatment, and therefore mTORC1 inhibition, would be a safe anti-aging approach or cause
51 excessive immunosuppression. Indeed, in rats, rapamycin inhibited wound healing (19) and in Tuberous
52 Sclerosis Complex patients, which have an aberrant hyperactivation of mTOR signaling, rapamycin led to
53 an increase in dermatologic adverse events such as oral ulceration and acneiform eruptions (20).

54 In this study, we aimed to understand how long-term, low-dose rapamycin could affect the ageing
55 immune system under both basal and inflammatory conditions. To this end, mice were given a low dose
56 of dietary rapamycin for a period of 5 months and immune cell proportions and inflammatory markers
57 were then measured at steady state and upon and LPS challenge. We found that long-term treatment did
58 not substantially alter immune cell populations, nonetheless, it counteracted the age-related increase of
59 IL-17 producing γδ T cells and moderately blunted peripheral and brain-related inflammation. Together,
60 our data reveal that long-term rapamycin treatment could be a potential intervention to modulate age-
61 associated IL-17-responses.

62 Results

63 Rapamycin does not alter myeloid cells skewing in aging

64 In order to assess the broad effect of long-term rapamycin exposure on aging of the immune system, we
65 designed a study to compare mice fed a rapamycin-containing diet (samples named "Old Rapa") vs mice
66 fed with a diet containing only the encapsulating compound EUDRAGIT® ("Old Eud"). The diet composition
67 and rapamycin dose were selected based on the original study by Zhang *et al.*, demonstrating lifespan
68 extension following rapamycin treatment (21). Mice were placed on the diet at 17-19 months and
69 assessed 5 months later. Three months old mice fed a standard diet were analyzed simultaneously for
70 comparison (**Fig 1A**).

71 Rapamycin-containing diet reduced mTORC1 signaling, as indicated by reduced phosphorylation of
72 ribosomal protein S6 (p-S6) in CD11b+ myeloid cells in the blood. The decrease in p-S6 levels was
73 comparable between two different cohorts, despite differences in age at the start of treatment (8 months

74 vs. 17–19 months), underlying that a similar extent of mTOR inhibition can be achieved at this dose and
75 treatment duration, irrespective of age **(Fig 1B)**.

76 In order to assess the effect of rapamycin on proportions of peripheral immune cells, we first assessed
77 mature myeloid cells by flow cytometry. Previous publications have highlighted that aging is associated
78 with alterations in immune homeostasis, notably, shifts to a higher myeloid cellular output also called
79 "myeloid skewing" (22-23).

80 At the study endpoint, blood, bone marrow, spleen, and peritoneal lavage were collected and the
81 percentage of Ly6C+/Ly6G– monocyte and Ly6C+/Ly6G+neutrophil populations was assessed (**Fig 1C**).
82 Monocyte and neutrophil proportions were quantified as percentage of live cells.

83 In our cohort, we did not observe an effect of rapamycin on monocyte or neutrophils in any of the tissues
84 investigated (**Fig 1D**) or an increase of the percentage of myeloid cells with age (**Fig 1D**).

85 These data collectively suggest that rapamycin does not exert any significant effect on monocytes and
86 neutrophils numbers, as their percentage in blood, bone marrow, peritoneal lavage and spleen in aged
87 mice was not affected.

88 Rapamycin does not affect B cell populations in older mice

89 We next investigated if a rapamycin-containing diet could impact the lymphoid lineage, focusing first on
90 B cells in the bone marrow, lymph nodes, peritoneal lavage, and blood (**Fig 2A**).

91 B-cell differentiation in the bone marrow was assessed by measuring cells expressing B220 and the μ-
92 chain of immunoglobulin M (IgM). No significant changes were observed in the proportions of pro-B cells,
93 pre-B cells and immature B cells (**Fig 2B**). However, although not statistically significant, we noted a trend
94 towards an increase in mature and transitional B cells in aged mice receiving rapamycin, resembling levels
95 observed in young mice (**Fig 2B**).

96 Regarding naïve B cells in lymph nodes and spleen, no substantial differences were noticed across the
97 three groups (**Fig 2C**).

98 Finally, we investigated B1 and B2 cell populations in the spleen and peritoneal lavage based on IgM,
99 CD11b and CD5 markers. Consistent with previous findings, no significant differences were detected
100 across B cell subpopulations, including subsets of B1 cells such as B1a and B1b, in the spleen and in the
101 peritoneal lavage (**Fig 2D**).

102 Altogether, these results indicate that low-dose rapamycin administration has a minimal impact on B cells
103 in aging.

104

Rapamycin-treated mice show minor changes in naïve and memory T-cell populations

Aging is associated with a decline in naïve T cell numbers and an increase in memory T cells (24, 25). In previous studies, rapamycin has been shown to increase differentiation of memory CD8 T cells (26, 27), however, mTOR-deficiency impairs differentiation of CD4 T cells to Th1, Th2 and Th17 subsets (28). Therefore, we assessed whether rapamycin treatment could influence the age-associated skewing of naïve to memory T cell populations. To this end, we assessed naïve (CD62L+CD44–), central (CD62L+CD44+) and effector memory (CD62L–CD44+) CD4 and CD8 T cells by measuring the expression of lymph node homing receptor, CD62L, a marker for naïve and central memory T cells, together with CD44, a marker of T cell memory and activation. Helper (CD4+) and cytotoxic (CD8+) T cells were assessed from lymph node, spleen and peritoneal lavage (**Fig 3A**).

CD4+ T cells isolated from lymph node and spleen of rapamycin-fed mice showed a slight increase in naïve T cells in lymph nodes and spleen, as well as in central memory CD4+ T cells in the spleen, although differences did not reach statistical significance.

No differences were observed for $CD8^+$ T cells in the lymph node, albeit an increase was observed in $CD8^+$ central memory T cells in the spleen of rapamycin-fed mice compared to both the young and old Eudragit groups (**Fig 3E**). This corroborates previous literature reporting that mTORC1 inhibition via rapamycin can induce an increase in the generation of CD8+ memory T cells (29).

In the peritoneal lavage, CD4+ T cells showed a switch from naïve to effector T cells (**Fig 3F&G**), which appeared specific to the rapamycin treatment. To a certain extent, CD8+ T cells in the peritoneal lavage showed a similar trend, although it did not reach statistical significance.

Overall, these data show modest changes in T cell populations and differentiation to CD8+ T memory cells following rapamycin treatment, in line with previous reports.

Rapamycin diet induces a decrease in IL-17-producing γδ T cells

While the effect of rapamycin on T cells expressing the main alpha/beta T cell receptor have been investigated, the effect on the less abundant gamma-delta T cell population, which express a type of T cell receptor that does not require MHC recognition, are not well described. In the context of cancer, rapamycin has been shown to enhance γδ T cell responses (30), however, the effect of long-term rapamycin administration on γδ T cell proportion remains unknown. For this reason, we next assessed whether rapamycin diet could have an effect on γδ T cell subsets.

Peritoneal γδ T cells are subdivided in IFN-γ- and IL-17-producing cells, distinguished by the expression of surface marker CD27 (31). CD3+, CD4–, CD8–, γδ TCR+, CD27+ and CD27– cells were assessed in the peritoneal lavage, as well as spleen and lymph node (**Fig 4**).

In the peritoneal lavage, CD27+ γδ T cells showed a decrease, while CD27– γδ T cells showed an increase with age (**Fig 4A&B**). In contrast, while rapamycin did not affect CD27+ γδ T cells, it significantly affected

140 the IL-17producing, CD27– counterparts, rescuing their levels to those observed in young mice (**Fig 4B**).
141 Similar trends were observed in the spleen and lymph nodes, although differences did not reach statistical
142 significance (**Fig 4C&D**).

143 Taken together, these data indicate that rapamycin prevents the increase in IL-17-secreting γδ T cells
144 that normally accompanies aging.

145

146 Rapamycin diet modulates microglia reactivity

147 Our data indicated that long-term rapamycin did not significantly affect the proportion of peripheral
148 immune cells, except for a clear effect on a subset of IL-17-producing γδ T cells.

149 Given these differences, we investigated whether systemic levels of inflammatory cytokines were also
150 altered (Schematic in **Fig 5A**). To this end, serum cytokine levels were assessed, however, we did not
151 observe any differences in serum concentration of IL-17A together with IL-6, IL-10, IL-27 (**Fig 5B**).

152 Nonetheless, since IL-17 levels can modulate neuroinflammation (32), we next investigated if the
153 rapamycin diet affected the phenotype of central nervous system (CNS) tissue resident immune cells,
154 microglia. To this end, we assessed the expression of pro-inflammatory cytokines and reactive microglial
155 markers using quantitative reverse transcription PCR (RT-qPCR) in microglia cells. Although aging is known
156 to induce upregulation of inflammatory cytokines and receptors in microglia, our data indicate that
157 rapamycin did not counteract age-associated neuroinflammation (**Fig 5C&D**).

158 Although no changes at steady state were observed, we reasoned that systemic and brain inflammation
159 might be affected in response to a strong inflammatory stimulus, such as intraperitoneal exposure to
160 lipopolysaccharide (LPS).

161 Thus, a separate cohort of mice were fed with either Eudragit or rapamycin diet from 6 months of age for
162 5 months, then challenged with 2 mg/kg of LPS intraperitoneally and serum cytokine levels and microglia
163 activation were analyzed 4 hours later.

164 Serum cytokines IL-1β, TNF-α, IL-23, IL-12p70, IFN-β, and IFN-γ were not different between the two diets
165 (**Fig 5E**). However, the inflammatory cytokines IL-12p40, IL-17A and IL-27 were significantly reduced in
166 rapamycin-fed mice upon LPS stimulation, along with the anti-inflammatory cytokine IL-10 (**Fig 5E**).

167 Examining the microglial response, we found that rapamycin administration moderately reduced
168 inflammatory markers *Tnf-α*, *Il6* and *Tlr2* gene expression while others, such as *Il-12a* and *Il-12b* remained
169 unaffected (**Fig 5F**).

170 Taken together, these results suggest that rapamycin diet can in part reduce systemic and brain
171 inflammation in response to a strong systemic inflammatory stimulus.

172

173 # Discussion

174 Hyperactivation of mTORC1 signaling has been associated with impaired metabolic health and reduced
175 longevity across multiple species, including mice and humans (33-34). The detrimental effects of sustained
176 mTORC1 activity may stem, at least in part, from remodeling of the immune landscape and its contribution
177 to inflammation (35). Accumulating evidence demonstrates that attenuation of mTORC1 activity
178 promotes healthy aging and extends lifespan (36–39). Nonetheless, the long-term consequences of
179 chronic, low-level mTORC1 inhibition on the immune system remain incompletely understood. To address
180 this, we tested the effect of low-dose, long-term rapamycin administration, based on the hypothesis that
181 the resulting mild mTORC1 inhibition could remodel the immune landscape of mice and fine-tune their
182 inflammatory status.

183 In this study, we investigated how the peripheral immune system and the brain tissue-resident
184 macrophages responded to a rapamycin-containing diet administered in adulthood (6-8months) or later
185 in life (17-19 months). Our findings demonstrate that the treatment was well tolerated and overall safe;
186 and while it did not induce major alterations in immune cell populations, it produced subtle yet significant
187 beneficial effects on immune function in old mice.

188 We first examined the impact of the rapamycin-containing diet on myeloid cell populations in an aged
189 cohort. Previous studies in adult mice have reported that rapamycin treatment can promote expansion of
190 myeloid cells (40) and reshape their transcriptome under chronic conditions (41). In contrast, in our study
191 of C57BL/6J mice, rapamycin supplementation did not significantly affect the abundance of myeloid cells
192 across multiple compartments. Regarding the lymphoid lineage, likewise we observed minimal effects on
193 the abundance of different subpopulations. However, we observed a downregulation of the CD27–, IL-17-
194 producing γδ T cells, more pronounced in the peritoneal lavage, where they have been implicated in
195 cancer (42) and bowel inflammation (43). The decrease in CD27– γδ T cells could be linked to the role of
196 mTORC1 in Th17 cell differentiation, mediated through the PI3K–mTORC1 axis (44–46).

197 As rapamycin has been proposed also as an anti-aging agent to preserve brain health and cognition, we
198 were particularly interested in assessing the effect of systemic mTORC1 inhibition on brain-resident
199 microglia. It is known that with age, microglia acquire a primed phenotype, characterized by increased
200 reactivity to an inflammatory stimulus (47). In this study, we demonstrated that rapamycin attenuates the
201 priming phenotype, since in response to a peripheral LPS challenge, the upregulation of inflammatory
202 cytokines and receptors was reduced. Although modest, this reduction could prove beneficial to
203 counteract brain inflammation that accompanies peripheral infections in the elderly (48). Our study did
204 not determine the mechanism underlying the reduction in microglia priming, particularly since rapamycin
205 does not efficiently cross the blood-brain barrier (49–51). However, reduced microglia reactivity is likely
206 either mediated by reduced systemic inflammation or by modulation of the gut-brain axis, driven by
207 rapamycin-induced alterations of the gut microbiome. Notably, even non-oral rapamycin treatment can
208 affect the gut microbial composition (52), a core component of the gut–brain axis that has been identified
209 as a contributor to alterations in microglial behavior (53-55). Indeed, upon LPS, we could observe
210 diminished levels of circulating pro-inflammatory cytokines, such as IL-27 and IL-17. On the other hand,
211 the immunomodulatory cytokine IL-10 was also decreased. This effect might be related to the decrease
212 in inflammatory cytokines inducing a weaker feedback signal that upregulates anti-inflammatory
213 responses (56).

214 Together, our results provide additional insights into how dietary rapamycin modulates the aged immune
215 system: the absence of major changes in immune cell composition, combined with evidence of beneficial
216 effects on CD27– γδ T cells, microglia and cytokine balance, supports the notion that rapamycin can be
217 administered safely without causing overt immunosuppression. This is particularly relevant given the
218 increasing clinical interest in rapamycin and rapalogs as geroprotective interventions (57, 58). Our data
219 highlight the need to carefully dissect tissue-specific and age-dependent responses to mTORC1 inhibition,
220 and they underscore that the beneficial effects of rapamycin in aging likely arise from subtle recalibrations
221 of immune and inflammatory networks rather than extensive immune remodeling, at least at the dose
222 investigated by us.

223 Further work is needed to determine whether these modest but significant immune effects translate into
224 improved resilience to age-related pathologies, including neuroinflammation, infections, and systemic
225 inflammation. Recent work suggest that peripheral immune signals may influence innate immune cells in
226 the aged brain: IL-17 produced by γδ T cells may act on IL-17 receptors expressed by microglia and
227 modulate their activation state (59). It has recently been shown that gut-derived γδ T17 cells migrate to
228 the meninges, where IL-17A can alter the mitochondrial function of microglia and trigger downstream
229 inflammatory pathways leading to microglial synaptic pruning in mouse models of encephalopathy (60).
230 This raises the intriguing possibility that dietary rapamycin may exert some of its effects on brain microglia
231 indirectly via modulation of peripheral γδ T cell responses, although further work is needed to test this
232 hypothesis in the context of aging. In summary, our findings contribute to a growing body of evidence
233 suggesting that dietary rapamycin is a safe and promising strategy for promoting healthy aging by
234 modulating the aged immune system.

235 Methods

236 Mice

237 C57BL6J female and male mice of different ages, as indicated in figure legends, were purchased from
238 Charles River and fed a chow rapamycin-containing diet for a period of 5 months. Mice were housed at
239 Barts Cancer Institute, Queen Mary University of London, UK and DZNE Bonn, Germany and experiments
240 were carried out under UK Home Office PPL 70/7411 and German TVA 81-02.04.2018.A215.

241 Rapamycin diet

242 Food-encapsulated rapamycin was prepared following the protocol by Harrison *et al*., (18).

243 Rapamycin was obtained from Rapamycin Holdings (now Entomora Biosciences) in San Antonio, Texas,
244 USA. Rapamycin was microencapsulated with an enteric coating material, Eudragit S100 (Röhm Pharma,
245 Germany), which protects rapamycin through the food preparation process. Since Eudragit S100 is water
246 soluble only at non-acidic pH, rapamycin is only released in the small intestine and protected in the
247 stomach. Eudragit-microencapsulated rapamycin and Eudragit as control were incorporated into separate
248 LabDiets on a 5058 base by Purina Labs. The amount of rapamycin used corresponded to 152 ppm,
249 resulting in a 14 ppm concentration of active rapamycin in mice (2.24 mg of rapamycin per kg body
250 weight).

251 **In vivo LPS injection**

252 Female 6-month-old mice were fed a rapamycin- or Eudragit-diet for 5 months, then injected with 2 mg/kg
253 of LPS of E coli 0111:B4 (Sigma, Cat. No. 297-473-0) in 200 µL PBS or PBS only as a control. Intraperitoneal
254 injections were performed using a 27G needle and 1 mL syringe. Mice were sacrificed after 4 hours and
255 organs were collected as described below.

256 **Organ processing**

257 *Blood*

258 Blood was obtained by cardiac puncture using a 27G needle and 1 mL syringe coated in 0.5 M
259 Ethylenediaminetetraacetic acid (EDTA). It was then transferred into a 1.5 mL EDTA-coated tube and
260 placed on ice before being centrifuged 3 times at increasing speed, removing pellets each time.
261 Centrifugation speeds were 200 x g for 3 min; 2,300 x g for 5 min and 16,100 x g for 3 min. Plasma was
262 then aliquoted and snap frozen before being stored at -80°C until cytokine assessment was carried out.

263 *Spleen*

264 Spleens were harvested, placed in 10 mL of PBS and kept on ice until further processing. Afterwards, they
265 were placed on a 70 µm cell strainer from Fisher Scientific (Cat. No. 11597522). They were gently mashed
266 through the strainer using a 5 mL syringe plunger. 10 mL of PBS was added to the cell suspension before
267 centrifugation at 300 x g for 10 minutes at 4°C.

268 *Bone marrow*

269 Cells were obtained from the bone marrow by flushing the femurs and tibia with Dulbecco's Modified
270 Eagle Medium (DMEM, Sigma, D5768) supplemented with 10% Fetal Bovine Serum (FBS, Life Technology,
271 Cat. No. 10500-064) and 1% penicillin/streptomycin (Sigma, Cat. No. P4333). 1 mL of complete media was
272 flushed through the bone marrow using a 27G needle, several times. Cells were then strained through a
273 70 µm cell strainer before 20 mL of PBS was added to the cell suspension and cells were spun at 300 x g
274 for 10 minutes 4°C.

275 *Brain*

276 The brain was dissected following perfusion with 35 mL of ice-cold Hank's balanced salt solution (HBSS)
277 for 5 minutes and subsequently digested using a neuronal dissociation kit (Miltenyi Biotec, Cat. No. 130-
278 092-628). Next, cells were washed twice in HBSS and myelin was removed by negative selection using
279 myelin removal beads (Miltenyi Biotec, 130-094-060) in MACS LS columns (Miltenyi Biotec, Cat. No. 140-
280 096-433). Briefly, 1.8 mL of fluorescence-activated cell sorting (FACS) buffer [phosphate buffered saline
281 (PBS) + 0.5% bovine serum albumin (BSA) + 2mM EDTA] and 200 µL of myelin removal beads were added
282 to each brain cell suspension and incubated at 4°C in the dark for 15 minutes. Following this incubation,
283 18 mL of FACS buffer was added to wash the cells, then centrifuged for 10 minutes at 300 x g. Using three
284 LS columns per brain, 1 of 3 mL of beads/cell suspension were loaded onto each column placed in a
285 QuadroMACS separator magnet (Miltenyi Biotec, Cat No. 130-042-302). This step was required to

286 separate bead-bound myelin from the cell suspension. Each LS column was washed twice with FACS buffer
287 and each time the flow-through was collected in order to collect brain cells.

288 **Cell processing for flow cytometry**

289 Cells from blood, spleen and bone marrow were first subjected to red blood cell lysis using 10X red blood
290 cell lysis buffer (eBioscience, Cat. No. 00-4300-54), diluted 1:10 in distilled water. Cell pellets were
291 resuspended in 10 mL of 1X lysis buffer and placed in the dark for 10 minutes at room temperature.
292 Following this incubation, cells were washed twice with FACSbuffer [phosphate buffered saline (PBS) +
293 0.5% bovine serum albumin (BSA) + 2mM EDTA] and used for subsequent antibody staining.

Target	Manufacturer	Cat Number	Clone	Dilution factor
CD4	eBioscience	17-0041-83	GK1.5	1:100
CD8	eBioscience	46-0081-80	53-6.7	1:100
CD45	eBioscience	9047-9459-120	2D1	1:100
CD62L	eBioscience	12-0621-85	MEL-14	1:100
CD11B	eBioscience	25-0112-82	M1/70	1:200
LY6C	eBioscience	48-5932-82	HK1.4	1:100
LY6G	eBioscience	17-5931-81	RB6-8C5	1:100
F4/80	eBioscience	11-4801-85	BM8	1:100
CLEC7A	eBioscience	17-5859-80	Bg1fpj	1:100
γδ TCR	Biolegend	118108	GL3	1:100
CD27	Biolegend	124216	LG.3A10	1:100
TLR2	eBioscience	12-9021-80	6C2	1:100
PS6	Cell Signaling	5018	N/A	1:50
DAPI	Cambridge Bioscience	40043-BT	N/A	2.5 µg/mL
FIXABLE VIABILITY DYE (FVD)	eBioscience	65-0863-18	N/A	1:200

294 *Tab. 1, List of antibodies and fluorescent dyes implemented in flow cytometry experiments.*

295 **Flow cytometry staining**

296 Cells were stained in 96-well V-bottom plates from Thermo Fisher (Cat.No. 2605), 2 x 10^6 cells in 100 µL
297 were added to each well and the plate was centrifuged at 300 x g for 5 minutes at 4°C. Cells were then
298 resuspended in 30 µL of CD16/CD32 FcR block (eBioscience, Cat. No. 14-0161-86) for 15 minutes at 4°C.
299 Following FcR block, a 2X antibody mix was prepared using FACS buffer and 30 µL was added to each well.
300 All relevant information regarding the panel of antibodies used (manufacturer, clone and dilutions) is
301 summarized in Tab. 1. After a 30 min incubation at 4°C in the dark, cells were washed twice with 150 µL
302 of FACS buffer before being resuspended in 150 µL of FACS buffer, which was transferred to 1.2 mL FACS
303 tubes (Star lab, Cat. No. I1412-7400). Data acquisition was carried out with a 4-laser LSRFortessa or a 5-
304 laser FACSymphony (BD Biosciences) and data analysis was done using FlowJo software (BD Bioscience).

305 **Microglia isolation**

306 Following brain homogenization (see Organ harvesting: Brain) single cell suspension was resuspended in
307 500 µL of FACS buffer and 40 µL of CD11b microbeads (Miltenyi Biotec, Cat. No. 130-093-636) and
308 incubated at 4°C in the dark for 15 minutes. Following this incubation, cells were washed with 3 mL of
309 FACS buffer and centrifuged for 10 min at 300 x g at 4°C. Using one MS column (Miltenyi Biotec, Cat. No.
310 130-042-201) per sample, 500 µL of bead/cells were loaded onto each column placed in an OctoMACS
311 separator magnet (Miltenyi Biotec, Cat. No. 130-042-108). Each MS column was washed twice with FACS
312 buffer and then 1 mL of FACS buffer was used to flush CD11b-positive cells using the plunger provided.
313 Purity of microglia was assessed by flow cytometry analysis by staining an aliquot of cells with the
314 microglia-specific markers CD11b and CD45 and reached 92-95%.

315 **RNA isolation**

316 Microglia (0.5-1 x 10^6) were lysed in 350 µL RLT lysis buffer (Qiagen, Cat. No. 74004) and stored at -80°C.
317 RNA was extracted with the RNeasy microkit from Qiagen (Cat. No. 74004), according to the manufacturer
318 guidelines.

319 **cDNA synthesis and Quantitative Real-Time Polymerase Chain Reaction (qPCR)**

320 Following RNA extraction, RNA was reverse transcribed into cDNA using the High-Capacity cDNA Reverse
321 Transcription kit from Applied Biosystems (Cat. No. 436-8814). Briefly, a master mix was prepared that
322 contained (per reaction): 1X RT buffer, 1X random hexamers, 4 mM dNTP, 1 µL of reverse transcriptase
323 (50 U/ml) and 2.2 µL of nuclease-free water. This master mix was added to the extracted RNA, contained
324 in 12 µL, for a final volume per reaction of 20 µL. All samples were then incubated in a thermocycler using
325 the following program; 25°C for 10 minutes, 37°C for 120 minutes, 85°C for 5 minutes and held at 4°C.
326 Following cDNA synthesis, 130 µL of nuclease-free water was added to each sample to dilute the enzymes
327 used in the cDNA synthesis. A master mix was then prepared for the qPCR for each gene of interest, which
328 included per reaction: 10 µL of Biorad iTaq master mix (Biorad, Cat. No. 436-814) and 1 µL of each FAM
329 labelled gene of interest. This master mix was added to a qPCR plate and 9 µL of diluted cDNA was added
330 to each corresponding well. The Step One Plus Real Time PCR machine from Applied Biosystems was used
331 to carry out the qPCR. The PCR program included an initial denaturation cycle that lasted for 10 minutes
332 at 95°C, followed by 40 cycles of amplification that included 15 seconds at 95°C and one minute at 60°C;
333 the last part of the program included one more cycle at 25°C for 15 seconds. All primers used are
334 summarized in Tab. 2.

Target gene	Manufacturer	Cat Number
Clec7a	Applied Biosystems	Mm01183349_m1
Tlr2	Applied Biosystems	Mm00442346_m1
Tnf-α	Applied Biosystems	Mm00443258_m1
Il-1b	Applied Biosystems	Mm00434228_m1
Il-12b	Applied Biosystems	Mm01288989_m1

335 *Tab. 2, List of primers implemented in Real Time qPCR analysis.*

336 **LEGENDplex**

337 Cytokine levels in serum or in microglia protein lysates were determined using the Legendplex mouse
338 inflammation 13-plex panel, (Biolegend, Cat. No. 740446); a bead-based assay that allows simultaneous
339 measurement of analytes based on cell size using flow cytometry. Specifically, the cytokines assessed were
340 IFN-β, IFN-γ, IL-1β, IL-6, IL-10, IL-12B, IL-17A, IL-27 and TNF-α. The assay was carried out in a 96-well plate
341 following manufacturers' instructions. For TNF and IL-6 measurements on microglia culture supernatants,
342 the BD OptEIA ELISA kits were used (BD Pharmingen, Cat. No. 558534, 555240) and the assay was carried
343 out according to manufacturers' guidelines.

344 **ELISA**

345 ELISA kits were obtained from BD Biosciences: IL-12p40 (Cat. No. 555165), IL-6 (Cat. No. 555240) and TNFα
346 (Cat. No. 558534). ELISA was performed according to the manufacturer's guidelines; however, half-surface
347 area 96-well plates were obtained from Corning Costar (Cat. No. 3690) and used for the assay. The wells
348 in these plates are half the volume of standard 96-well plates, allowing the use of a reduced number of
349 samples and reagents. This was particularly important for plasma cytokine levels, as the amount of plasma
350 obtained from each mouse was potentially a limiting factor. Briefly, capture antibody was diluted in PBS
351 and added to each well of a 96-well plate. The plate was then incubated overnight at 4°C, prior to being
352 washed three times with wash buffer (PBS with 0.05% Tween-20). The plate was then incubated with
353 assay diluent (PBS with 10% FBS) for 1 hour, in order to block non-specific binding and washed three times
354 with wash buffer. The higher concentration of standards (1000 pg/mL) were made using a stock solution
355 of each cytokine and then a serial dilution was performed on a separate plate to obtain the remaining
356 standards (500, 250, 125, 62.5, 31.3 and 15.6 pg/mL). Samples and standards were then added to the
357 ELISA plate and incubated for 2 hours at room temperature. Samples that required dilution were diluted
358 in assay diluent. Following incubation, the plate was washed 5 times with wash buffer and then the
359 working detector solution (detection antibody and HRP) was added to the plate and it was incubated at
360 room temperature for 1 hour. The plate was then washed 7 times before the substrate solution
361 [Tetramethylbenzidine (TMB) and hydrogen peroxide from the TMB Substrate Reagent Set (BD
362 PHarmingen, Cat. No.555214)] was added and incubated in the dark for a maximum of 30 minutes.
363 Following the appropriate color change, 25 ml of 1M H3PO4 was added to stop the reaction. Plates were
364 analyzed on a plate reader plate reader to read the optical density at 450 nm.

365 **Statistical analysis**

366 Statistical analysis was conducted used GraphPad Prism, one-way ANOVA and Welch's t-test were
367 employed as required and as reported in the respective figure legends. A p value < 0.05 was considered
368 statistically significant. P values below 0.1 are reported in the figures.

369 # Figure Legends

370

371 **Figure 1. Long- term, low-dose rapamycin does not alter the proportion of myeloid cells.** (**A**) Schematic
372 model of young and old mice exposed to rapamycin diet with subsequent flow cytometry analysis of

373 immune myeloid cells. (**B**) p-S6 levels in CD11b+ cells from blood of old Eudragit and rapamycin mice,
374 pooled from two independent cohorts. The first cohort is represented in panel (**A**), in the second cohort,
375 treatment was initiated at 8 months of age and mice were analyzed at 13 months. (**C**) Representative
376 gating strategy for live cells expressing Ly6C and Ly6G to identify monocytes and neutrophils (n = 3–4 per
377 group). (**D**) Monocytes and neutrophil populations from blood, bone marrow, peritoneal lavage and
378 spleen from young, old Eudragit and old rapamycin mice, (n = 3–4 per group). Data are shown as
379 mean ± s.e.m. Statistical analysis was conducted by Welch's t-test (**B**) and One-way ANOVA (**D**).

380

381 **Figure 2. Rapamycin does not significantly alter B cell subsets, but shows a trend toward rescuing**
382 **transitional and mature B cells in aged mice.** (**A**) Schematic representation of the experimental setup. (**B**)
383 Representative flow cytometry gating strategy for bone marrow B cell subsets and their quantification (n
384 = 3–4 per group). (**C**) Representative gating strategy and quantification of naïve B cells from lymph nodes
385 and spleen (n = 3–4 per group). (**D**) Representative gating strategy and quantification of B1 and B2 cells,
386 including B1a and B1b subsets, from peritoneal lavage (n = 3–4 per group). Data are presented as mean ±
387 s.e.m. Statistical analysis was conducted by One-way ANOVA.

388

389 **Figure 3. Dietary rapamycin has minor effects on CD4+ and CD8+ T cell populations in aged mice.**

390 (**A**) Representative flow cytometry gating strategy for T cells. Gating was performed sequentially on FSC-
391 A versus SSC-A, singlets, live cells, and CD3+ cells, as shown in Fig. 4A (n = 3–4 per group). (**B–G**)
392 Quantification of CD62L and CD44 expression in CD4+ and CD8+ T cells from lymph nodes, spleen, and
393 peritoneal lavage (n = 3–4 per group). Data are presented as mean ± s.e.m. Statistical analysis was
394 performed by One-way ANOVA.

395

396 **Figure 4. Rapamycin prevents age-associated increase in IL-17-producing γδ T cells.** (**A**) Representative
397 flow cytometry gating strategy for identification of γδ T cells. (**B–D**) Quantification of CD27+ and CD27–
398 γδ T cells in the peritoneal lavage, spleen, and lymph nodes of aged mice (n = 3–4 per group). Data are
399 presented as mean ± s.e.m. Statistical analysis was conducted by One-way ANOVA.

400

401 **Figure 5. Rapamycin diet reduces inflammation in aged mice challenged with LPS.** (**A**) Schematic of young
402 and aged mice fed a control or rapamycin-supplemented diet, with or without LPS stimulation, followed
403 by RT-qPCR and flow cytometry analysis of myeloid immune cells. (**B**) Serum cytokines concentrations in
404 basal conditions. (**C-D**) Basal expression of inflammatory cytokines and receptors in microglia under
405 unstimulated conditions (n = 3 per group). (**E**) Serum cytokine concentrations in LPS-treated mice (n = 7
406 per group). (**F**) Expression of inflammatory cytokines in microglia following LPS stimulation (n = 8–9 per
407 group). Data are presented as mean ± s.e.m. Statistical analysis was conducted by Welch's t-test (**B, E, F**)
408 and One-way ANOVA (**C&D**).

409

410 ## Acknowledgements

411 We thank Profs Frances Balkwill and Federica Marelli-Berg (Queen Mary University of London) and Dr
412 Dan Ehninger (DZNE, Bonn) for useful discussions. We also thank previous and current members of the
413 Capasso group for experimental support.

414

415 ## Bibliography

416 1. Gilbert SF. Aging: The Biology of Senescence. In: Developmental Biology 6th edition [Internet].
417 Sinauer Associates; 2000 [cited 2024 July 17]. Available from:
418 https://www.ncbi.nlm.nih.gov/books/NBK10041/

419 2. López-Otín C, Blasco MA, Partridge L, Serrano M, Kroemer G. The Hallmarks of Aging. Cell. 2013 June
420 6;153(6):1194–217.

421 3. Papadopoli D, Boulay K, Kazak L, Pollak M, Mallette FA, Topisirovic I, et al. mTOR as a central
422 regulator of lifespan and aging. F1000Res. 2019 July 2;8:F1000 Faculty Rev-998.

423 4. Heitman J, Movva NR, Hall MN. Targets for cell cycle arrest by the immunosuppressant rapamycin in
424 yeast. Science. 1991 Aug 23;253(5022):905–9.

425 5. Wullschleger S, Loewith R, Hall MN. TOR Signaling in Growth and Metabolism. Cell. 2006 Feb
426 10;124(3):471–84.

427 6. Wang X, Proud CG. The mTOR Pathway in the Control of Protein Synthesis. Physiology. 2006
428 Oct;21(5):362–9.

429 7. Panwar V, Singh A, Bhatt M, Tonk RK, Azizov S, Raza AS, et al. Multifaceted role of mTOR
430 (mammalian target of rapamycin) signaling pathway in human health and disease. Sig Transduct
431 Target Ther. 2023 Oct 2;8(1):1–25.

432 8. Neff F, Flores-Dominguez D, Ryan DP, Horsch M, Schröder S, Adler T, et al. Rapamycin extends
433 murine lifespan but has limited effects on aging. J Clin Invest. 2013 Aug;123(8):3272–91.

434 9. Zou Z, Tao T, Li H, Zhu X. mTOR signaling pathway and mTOR inhibitors in cancer: progress and
435 challenges. Cell & Bioscience. 2020 Mar 10;10(1):31.

436 10. Kaldirim M, Lang A, Pfeiler S, Fiegenbaum P, Kelm M, Bönner F, et al. Modulation of mTOR Signaling
437 in Cardiovascular Disease to Target Acute and Chronic Inflammation. Front Cardiovasc Med. 2022
438 June 29;9:907348.

439 11. Li J, Kim SG, Blenis J. Rapamycin: One Drug, Many Effects. Cell Metabolism. 2014 Mar 4;19(3):373–9.

440 12. Hahn D, Hodson EM, Hamiwka LA, Lee VW, Chapman JR, Craig JC, et al. Target of rapamycin
441 inhibitors (TOR-I; sirolimus and everolimus) for primary immunosuppression in kidney transplant
442 recipients. Cochrane Database Syst Rev. 2019 Dec 16;12(12):CD004290.

443 13. Weichhart T, Costantino G, Poglitsch M, Rosner M, Zeyda M, Stuhlmeier KM, et al. The TSC-mTOR
444 signaling pathway regulates the innate inflammatory response. Immunity. 2008 Oct 17;29(4):565–
445 77.

446 14. Linke M, Pham HTT, Katholnig K, Schnöller T, Miller A, Demel F, et al. Chronic signaling via the
447 metabolic checkpoint kinase mTORC1 induces macrophage granuloma formation and marks
448 sarcoidosis progression. Nat Immunol. 2017 Mar;18(3):293–302.

449 15. Mannick JB, Morris M, Hockey HUP, Roma G, Beibel M, Kulmatycki K, et al. TORC1 inhibition
450 enhances immune function and reduces infections in the elderly. Science Translational Medicine.
451 2018 July 11;10(449):eaaq1564.

452 16. Netti GS, Infante B, Troise D, Mercuri S, Panico M, Spadaccino F, et al. mTOR inhibitors improve both
453 humoral and cellular response to SARS-CoV-2 messenger RNA BNT16b2 vaccine in kidney transplant
454 recipients. Am J Transplant. 2022 May;22(5):1475–82.

455 17. Mannick JB, Lamming DW. Targeting the biology of aging with mTOR inhibitors. Nat Aging. 2023
456 June;3(6):642–60.

457 18. Harrison DE, Strong R, Sharp ZD, Nelson JF, Astle CM, Flurkey K, et al. Rapamycin fed late in life
458 extends lifespan in genetically heterogeneous mice. Nature. 2009 July 16;460(7253):392–5.

459 19. Ekici Y, Emiroglu R, Ozdemir H, Aldemir D, Karakayali H, Haberal M. Effect of Rapamycin on Wound
460 Healing: An Experimental Study. Transplantation Proceedings. 2007 May 1;39(4):1201–3.

461 20. Pithadia DJ, Treichel AM, Jones AM, Julien-Williams P, Machado T, Moss J, et al. Dermatologic
462 adverse events associated with use of oral mechanistic target of rapamycin inhibitors in a cohort of
463 individuals with tuberous sclerosis complex. Br J Dermatol. 2020 Sept;183(3):588–9.

464 21. Zhang Y, Bokov A, Gelfond J, Soto V, Ikeno Y, Hubbard G, et al. Rapamycin extends life and health in
465 C57BL/6 mice. J Gerontol A Biol Sci Med Sci. 2014 Feb;69(2):119–30.

466 22. Ho YH, Del Toro R, Rivera-Torres J, Rak J, Korn C, García-García A, et al. Remodeling of Bone Marrow
467 Hematopoietic Stem Cell Niches Promotes Myeloid Cell Expansion during Premature or Physiological
468 Aging. Cell Stem Cell. 2019 Sept;25(3):407-418.e6.

469 23. Su TY, Hauenstein J, Somuncular E, Dumral Ö, Leonard E, Gustafsson C, et al. Aging is associated
470 with functional and molecular changes in distinct hematopoietic stem cell subsets. Nat Commun
471 [Internet]. 2024 Sept 11 [cited 2025 July 7];15(1). Available from:
472 https://www.nature.com/articles/s41467-024-52318-1

473 24. Quinn KM, Vicencio DM, La Gruta NL. The paradox of aging: Aging-related shifts in T cell function
474 and metabolism. Seminars in Immunology. 2023 Nov;70:101834.

475 25. Becklund BR, Purton JF, Ramsey C, Favre S, Vogt TK, Martin CE, et al. The aged lymphoid tissue
476 environment fails to support naïve T cell homeostasis. Sci Rep. 2016 Aug 2;6(1):30842.

477 26. Araki K, Turner AP, Shaffer VO, Gangappa S, Keller SA, Bachmann MF, et al. mTOR regulates memory
478 CD8 T-cell differentiation. Nature. 2009 July;460(7251):108–12.

479 27. Jung JW, Veitch M, Bridge JA, Overgaard NH, Cruz JL, Linedale R, et al. Clinically-Relevant Rapamycin
480 Treatment Regimens Enhance CD8+ Effector Memory T Cell Function In The Skin and Allow their
481 Infiltration into Cutaneous Squamous Cell Carcinoma. Oncoimmunology. 2018 July
482 30;7(9):e1479627.

483 28. Delgoffe GM, Kole TP, Zheng Y, Zarek PE, Matthews KL, Xiao B, et al. The mTOR Kinase Differentially
484 Regulates Effector and Regulatory T Cell Lineage Commitment. Immunity. 2009 June 19;30(6):832–
485 44.

486 29. He S, Kato K, Jiang J, Wahl DR, Mineishi S, Fisher EM, et al. Characterization of the Metabolic
487 Phenotype of Rapamycin-Treated CD8+ T Cells with Augmented Ability to Generate Long-Lasting
488 Memory Cells. Matloubian M, editor. PLoS ONE. 2011 May 17;6(5):e20107.

489 30. Dao V, Liu Y, Pandeswara S, Svatek RS, Gelfond JA, Liu A, et al. Immune-Stimulatory Effects of
490 Rapamycin Are Mediated by Stimulation of Antitumor γδ T Cells. Cancer Res. 2016 Oct
491 13;76(20):5970–82.

492 31. Ribot JC, deBarros A, Pang DJ, Neves JF, Peperzak V, Roberts SJ, et al. CD27 is a thymic determinant
493 of the balance between interferon-gamma- and interleukin 17-producing gammadelta T cell
494 subsets. Nat Immunol. 2009 Apr;10(4):427–36.

495 32. Park SE, Ferreira AFF, Kwon H, Yu J, Diniz L, Ulrich H, et al. The role of interleukin-17 in neurological
496 disorders. Animal Cells and Systems. 2025 Dec 31;29(1):372–86.

497 33. He D, Wu H, Xiang J, Ruan X, Peng P, Ruan Y, et al. Gut stem cell aging is driven by mTORC1 via a p38
498 MAPK-p53 pathway. Nat Commun. 2020 Jan 2;11(1):37.

499 34. Zarzycka W, Kobak KA, King CJ, Peelor FF, Miller BF, Chiao YA. Hyperactive mTORC1/4EBP1 signaling
500 dysregulates proteostasis and accelerates cardiac aging. Geroscience. 2025 Apr;47(2):1823–36.

501 35. Keane L, Antignano I, Riechers SP, Zollinger R, Dumas AA, Offermann N, Bernis ME, Russ J,
502 Graelmann F, McCormick PN, Esser J, Tejera D, Nagano A, Wang J, Chelala C, Biederbick Y, Halle A,
503 Salomoni P, Heneka MT, Capasso M. mTOR-dependent translation amplifies microglia priming in
504 aging mice. J Clin Invest. 2021 Jan 4;131(1):e132727.

505 36. Kapahi P, Zid BM, Harper T, Koslover D, Sapin V, Benzer S. Regulation of Lifespan in *Drosophila* by
506 Modulation of Genes in the TOR Signaling Pathway. Current Biology. 2004 May 25;14(10):885–90.

507 37. Mannick JB, Del Giudice G, Lattanzi M, Valiante NM, Praestgaard J, Huang B, et al. mTOR inhibition
508 improves immune function in the elderly. Science Translational Medicine. 2014 Dec
509 24;6(268):268ra179-268ra179.

510 38. Ortega-Molina A, Lebrero-Fernández C, Sanz A, Calvo-Rubio M, Deleyto-Seldas N, de Prado-Rivas L,
511 et al. A mild increase in nutrient signaling to mTORC1 in mice leads to parenchymal damage,
512 myeloid inflammation and shortened lifespan. Nat Aging. 2024 Aug;4(8):1102–20.

513 39. Joseph GA, Wang SX, Jacobs CE, Zhou W, Kimble GC, Tse HW, et al. Partial Inhibition of mTORC1 in
514 Aged Rats Counteracts the Decline in Muscle Mass and Reverses Molecular Signaling Associated
515 with Sarcopenia. Mol Cell Biol. 2019 Oct 1;39(19):e00141-19.

516 40. Li M, Lan Y, Gao J, Yuan S, Hou S, Guo T, et al. Rapamycin Promotes the Expansion of Myeloid Cells
517 by Increasing G-CSF Expression in Mesenchymal Stem Cells. Front Cell Dev Biol. 2022 Mar
518 17;10:779159.

519 41. Hurez V, Dao V, Liu A, Pandeswara S, Gelfond J, Sun L, et al. Chronic mTOR inhibition in mice with
520 rapamycin alters T, B, myeloid, and innate lymphoid cells and gut flora and prolongs life of
521 immune-deficient mice. Aging Cell. 2015 Dec;14(6):945–56.

522 42. Rei M, Gonçalves-Sousa N, Lança T, Thompson RG, Mensurado S, Balkwill FR, et al. Murine CD27(−)
523 Vγ6(+) γδ T cells producing IL-17A promote ovarian cancer growth via mobilization of protumor
524 small peritoneal macrophages. Proceedings of the National Academy of Sciences. 2014 Aug
525 26;111(34):E3562–70.

526 43. Nanno M, Kanari Y, Naito T, Inoue N, Hisamatsu T, Chinen H, et al. Exacerbating Role of γδ T Cells in
527 Chronic Colitis of T-Cell Receptor α Mutant Mice. Gastroenterology. 2008 Feb 1;134(2):481–90.

528 44. Kurebayashi Y, Nagai S, Ikejiri A, Ohtani M, Ichiyama K, Baba Y, et al. PI3K-Akt-mTORC1-S6K1/2 Axis
529 Controls Th17 Differentiation by Regulating Gfi1 Expression and Nuclear Translocation of RORγ. Cell
530 Reports. 2012 Apr 19;1(4):360–73.

531 45. Delgoffe GM, Kole TP, Zheng Y, Zarek PE, Matthews KL, Xiao B, et al. The mTOR Kinase Differentially
532 Regulates Effector and Regulatory T Cell Lineage Commitment. Immunity. 2009 June 19;30(6):832–
533 44.

534 46. Delgoffe GM, Pollizzi KN, Waickman AT, Heikamp E, Meyers DJ, Horton MR, et al. The kinase mTOR
535 regulates the differentiation of helper T cells through the selective activation of signaling by
536 mTORC1 and mTORC2. Nat Immunol. 2011 Apr;12(4):295–303.

537 47. Perry VH, Holmes C. Microglial priming in neurodegenerative disease. Nat Rev Neurol. 2014
538 Apr;10(4):217–24.

539 48. Sparkman NL, Johnson RW. Neuroinflammation Associated with Aging Sensitizes the Brain to the
540 Effects of Infection or Stress. Neuroimmunomodulation. 2008;15(4–6):323–30.

541 49. Cai S, Yuan Z, Chen Y, Gong M, Lai J, Yan P, et al. Transferrin and Borneol-Enhanced Liposomes for
542 Targeted Rapamycin Delivery in TBI. Int J Nanomedicine. 2025 Apr 11;20:4503–18.

543 50. Gonzales MM, Garbarino VR, Kautz TF, Song X, Lopez-Cruzan M, Linehan L, et al. Rapamycin
544 treatment for Alzheimer's disease and related dementias: a pilot phase 1 clinical trial. Commun
545 Med. 2025 May 20;5(1):189.

546 51. Mandrioli J, D'Amico R, Zucchi E, De Biasi S, Banchelli F, Martinelli I, et al. Randomized, double-blind,
547 placebo-controlled trial of rapamycin in amyotrophic lateral sclerosis. Nat Commun. 2023 Aug
548 17;14(1):4970.

549 52. Wu L, Kensiski A, Gavzy SJ, Lwin HW, Song Y, France MT, et al. Rapamycin immunomodulation
550 utilizes time-dependent alterations of lymph node architecture, leukocyte trafficking, and gut
551 microbiome. JCI Insight [Internet]. 2025 Apr 22 [cited 2026 Jan 9];10(8). Available from:
552 https://insight.jci.org/articles/view/186505

553 53. Antignano I, Liu Y, Offermann N, Capasso M. Aging microglia. Cell Mol Life Sci. 2023 Apr
554 21;80(5):126.

555 54. Huang Y, Wu J, Zhang H, Li Y, Wen L, Tan X, et al. The gut microbiome modulates the transformation
556 of microglial subtypes. Mol Psychiatry. 2023 Apr;28(4):1611–21.

557 55. Keane L, Clarke G, Cryan JF. A role for microglia in mediating the microbiota–gut–brain axis. Nat Rev
558 Immunol. 2025 Nov;25(11):847–61.

559 56. Brown CY, Lagnado CA, Vadas MA, Goodall GJ. Differential Regulation of the Stability of Cytokine
560 mRNAs in Lipopolysaccharide-activated Blood Monocytes in Response to Interleukin-10*. Journal of
561 Biological Chemistry. 1996 Aug 16;271(33):20108–12.

562 57. Lamming DW, Ye L, Sabatini DM, Baur JA. Rapalogs and mTOR inhibitors as anti-aging therapeutics. J
563 Clin Invest. 2013 Mar 1;123(3):980–9.

564 58. Mannick JB, Teo G, Bernardo P, Quinn D, Russell K, Klickstein L, et al. Targeting the biology of ageing
565 with mTOR inhibitors to improve immune function in older adults: phase 2b and phase 3
566 randomised trials. The Lancet Healthy Longevity. 2021 May 1;2(5):e250–62.

567 59. Wendeln AC, Degenhardt K, Kaurani L, Gertig M, Ulas T, Jain G, et al. Innate immune memory in the
568 brain shapes neurological disease hallmarks. Nature. 2018 Apr;556(7701):332–8.

569 60. Wu Y, Zhang Y, Yu Y, Wang X, Zhen Z, Yuan Y, et al. Small intestinal γδ T17 cells promote SAE
570 through STING/C1q-induced microglial synaptic pruning in male mice. Nat Commun. 2025 July
571 23;16(1):6779.

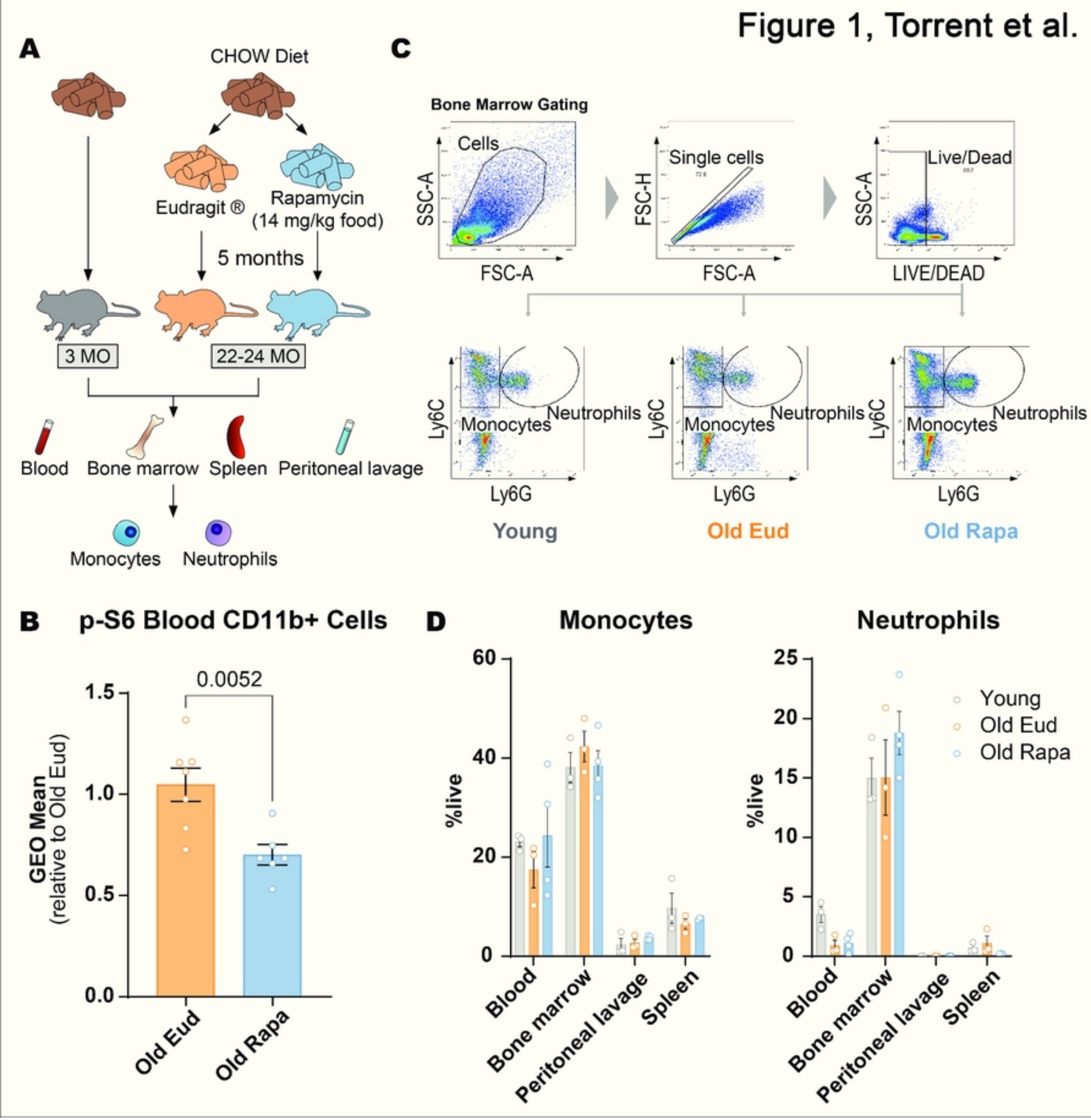
Figure 1, Torrent et al.
A
CHOW Diet
Eudragit ®
Rapamycin
(14 mg/kg food)
5 months
3 MO
22-24 MO
Blood
Bone marrow
Spleen
Peritoneal lavage
Monocytes
Neutrophils
C
Bone Marrow Gating
Cells
SSC-A
FSC-A
Single cells
FSC-H
FSC-A
Live/Dead
SSC-A
LIVE/DEAD
Ly6C
Ly6G
Monocytes
Neutrophils
Young
Old Eud
Old Rapa
B
p-S6 Blood CD11b+ Cells
0.0052
GEO Mean
(relative to Old Eud)
1.5
1.0
0.5
0.0
Old Eud
Old Rapa
D
Monocytes
Neutrophils
%live
60
40
20
0
25
20
15
10
5
0
Young
Old Eud
Old Rapa
Blood
Bone marrow
Peritoneal lavage
Spleen

Figure 1

Figure 3, Torrent et al.

A Gating strategy Naive and Memory T cells

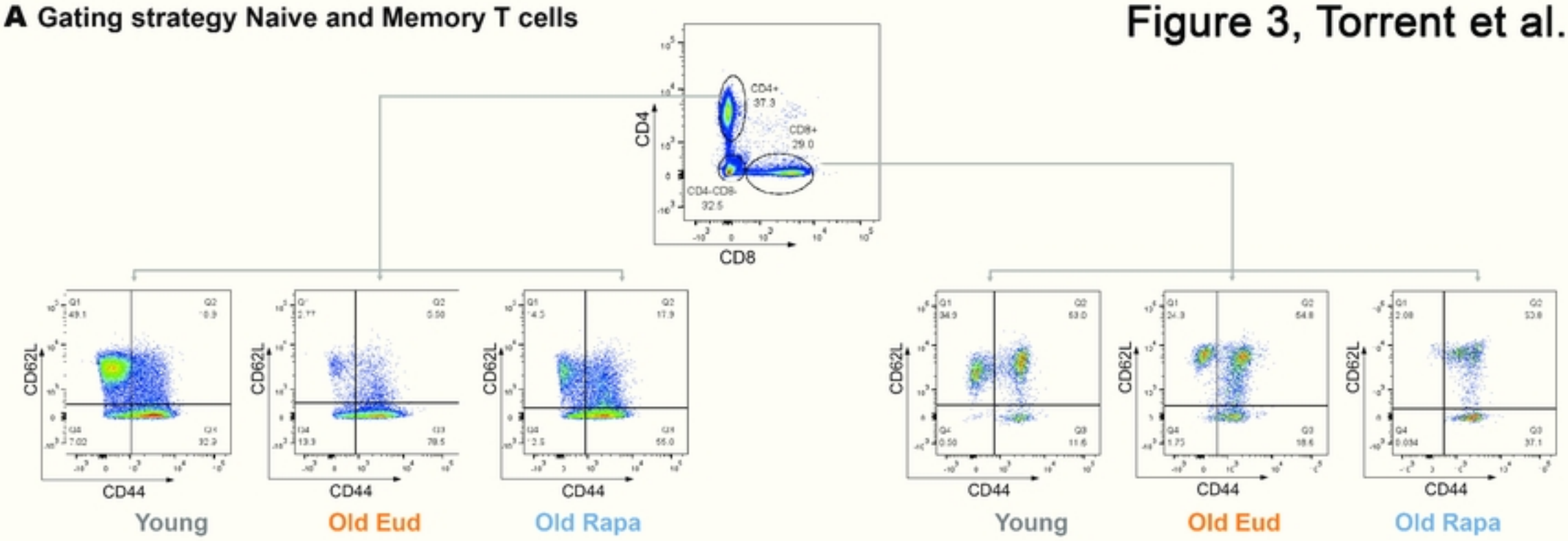

B Lymph Node

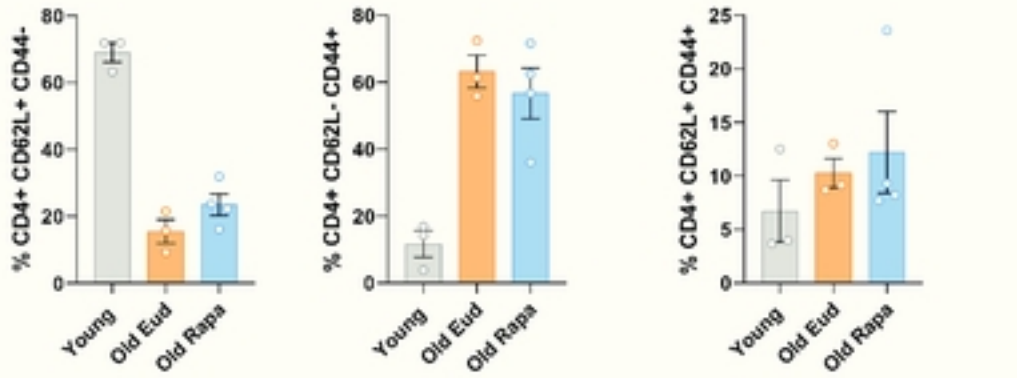

C Lymph Node

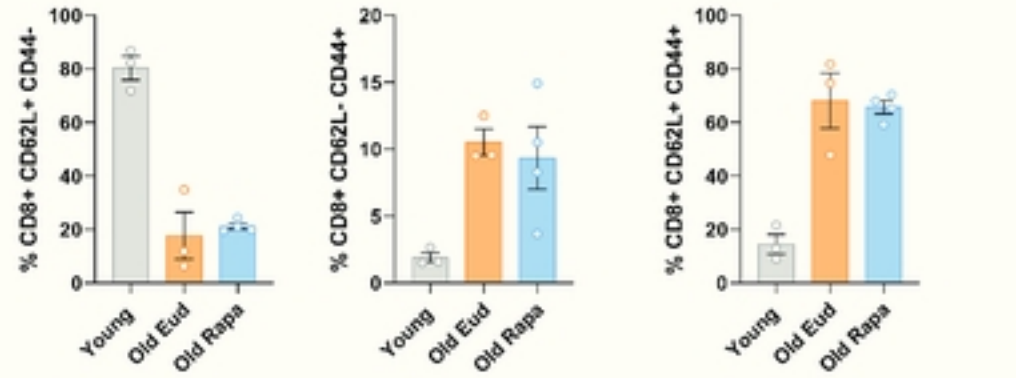

D Spleen

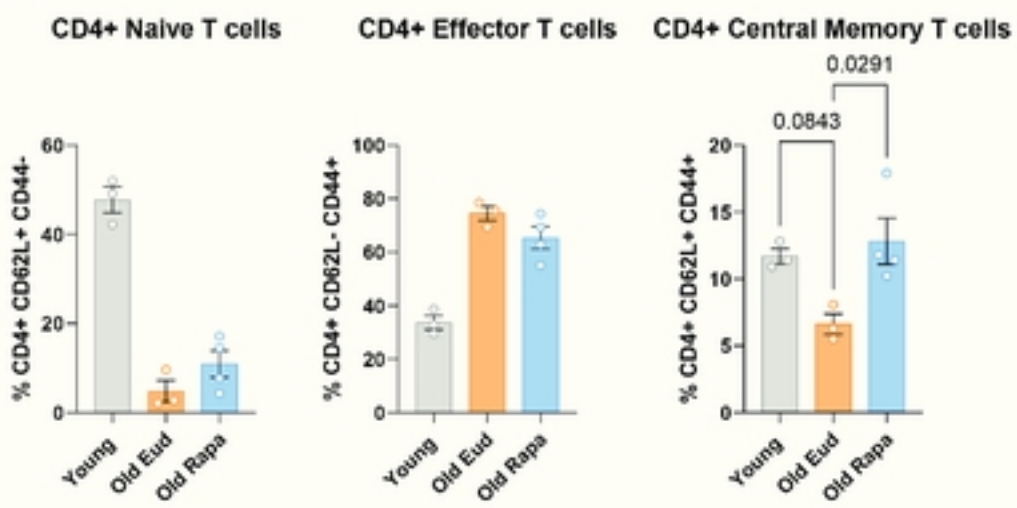

E Spleen

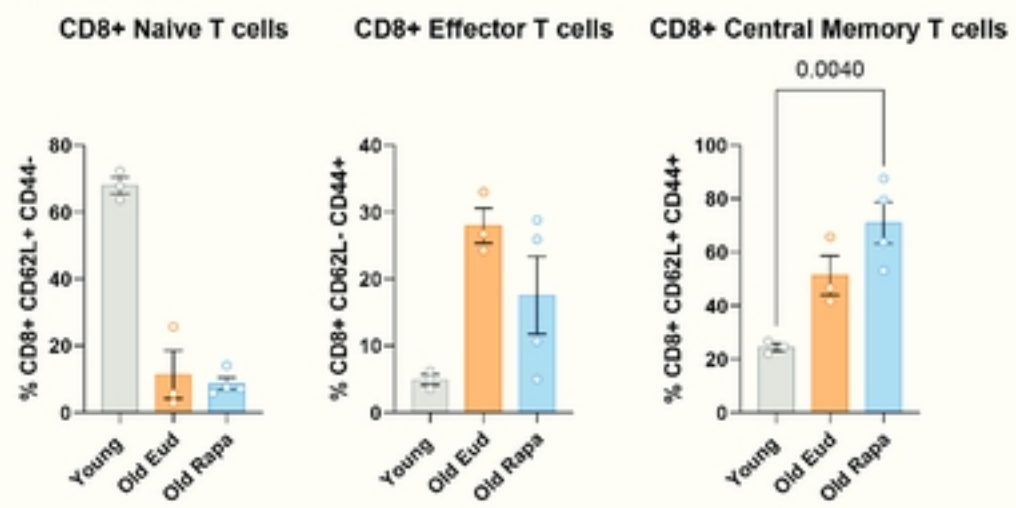

F Peritoneal Lavage

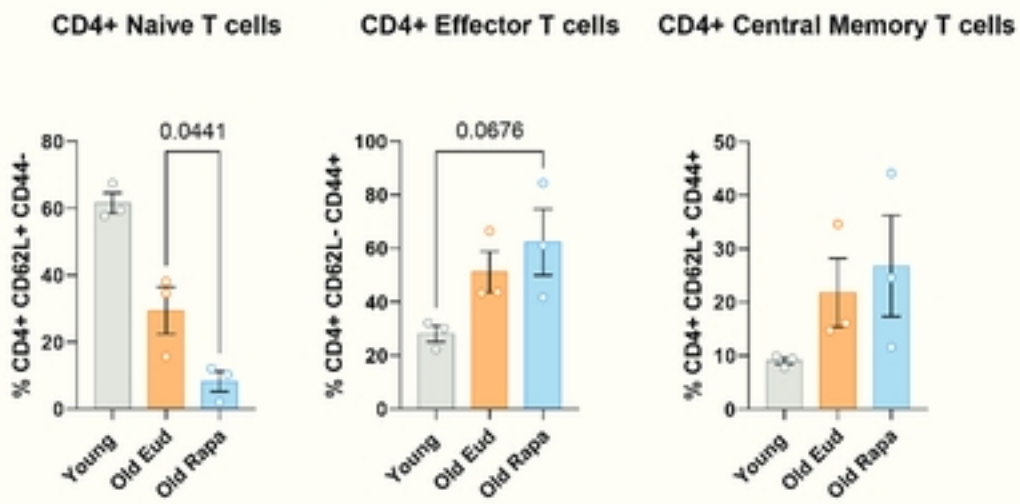

G Peritoneal Lavage

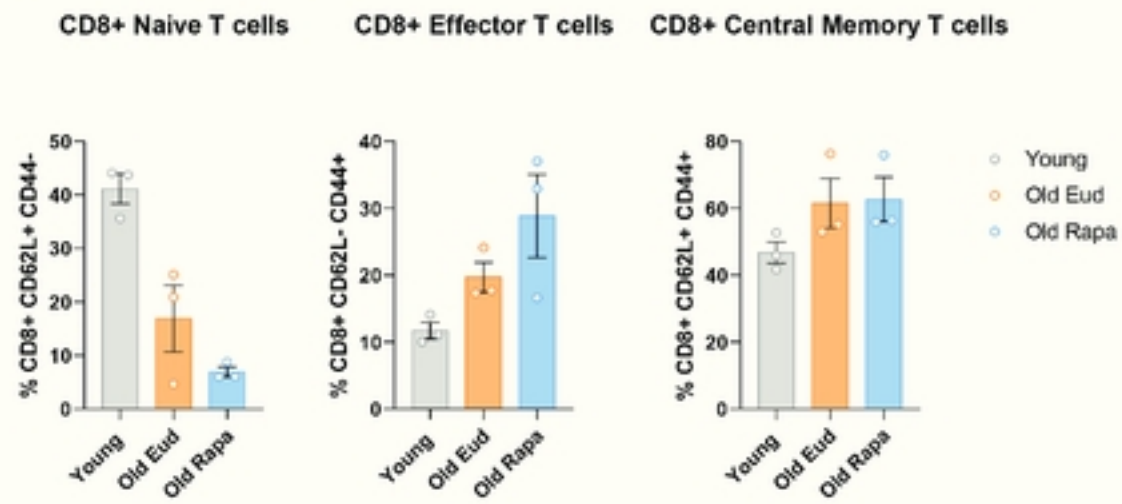

Figure 3

Figure 5, Torrent et al.

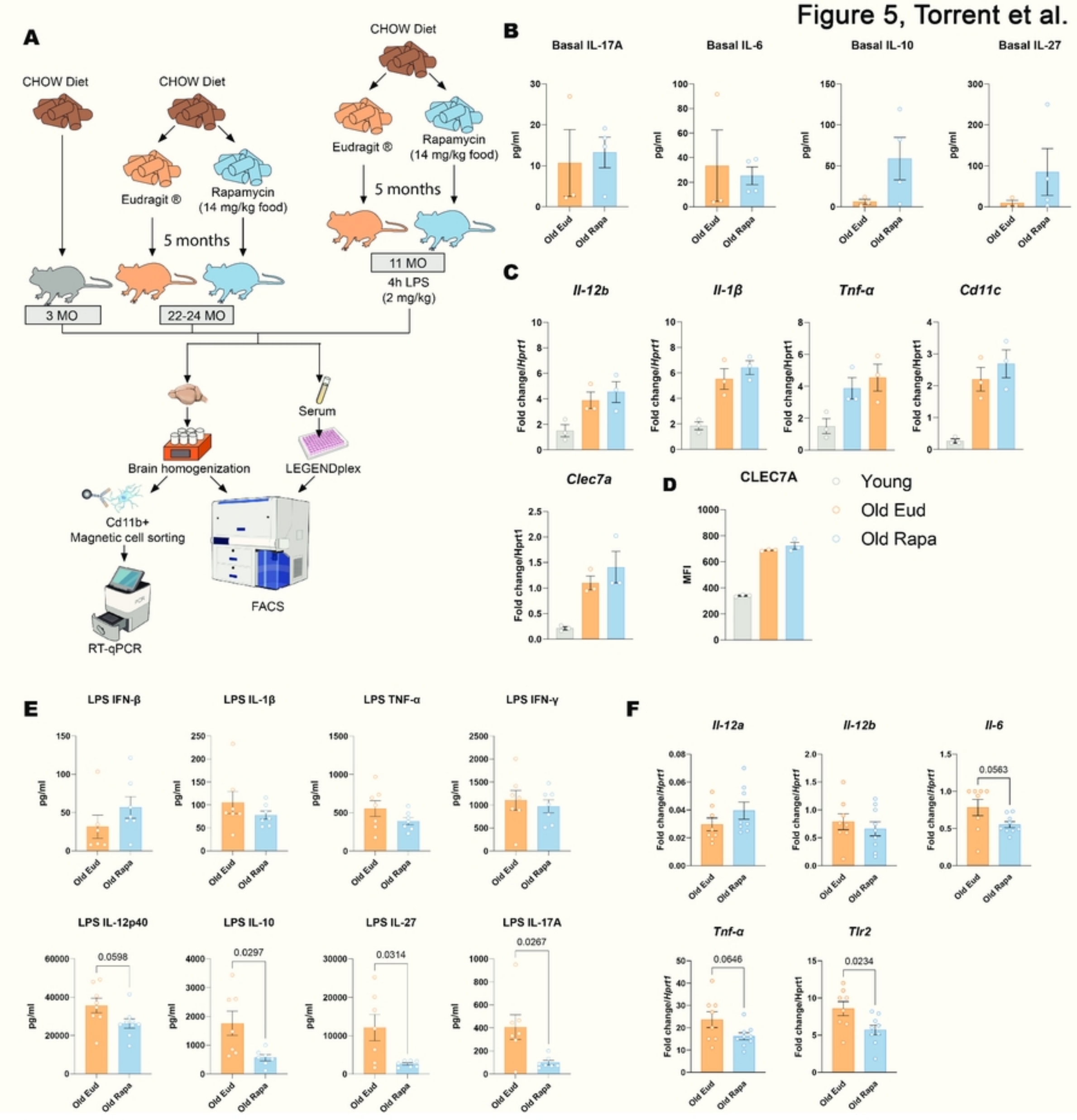

Figure 5

Figure 2, Torrent *et al.*

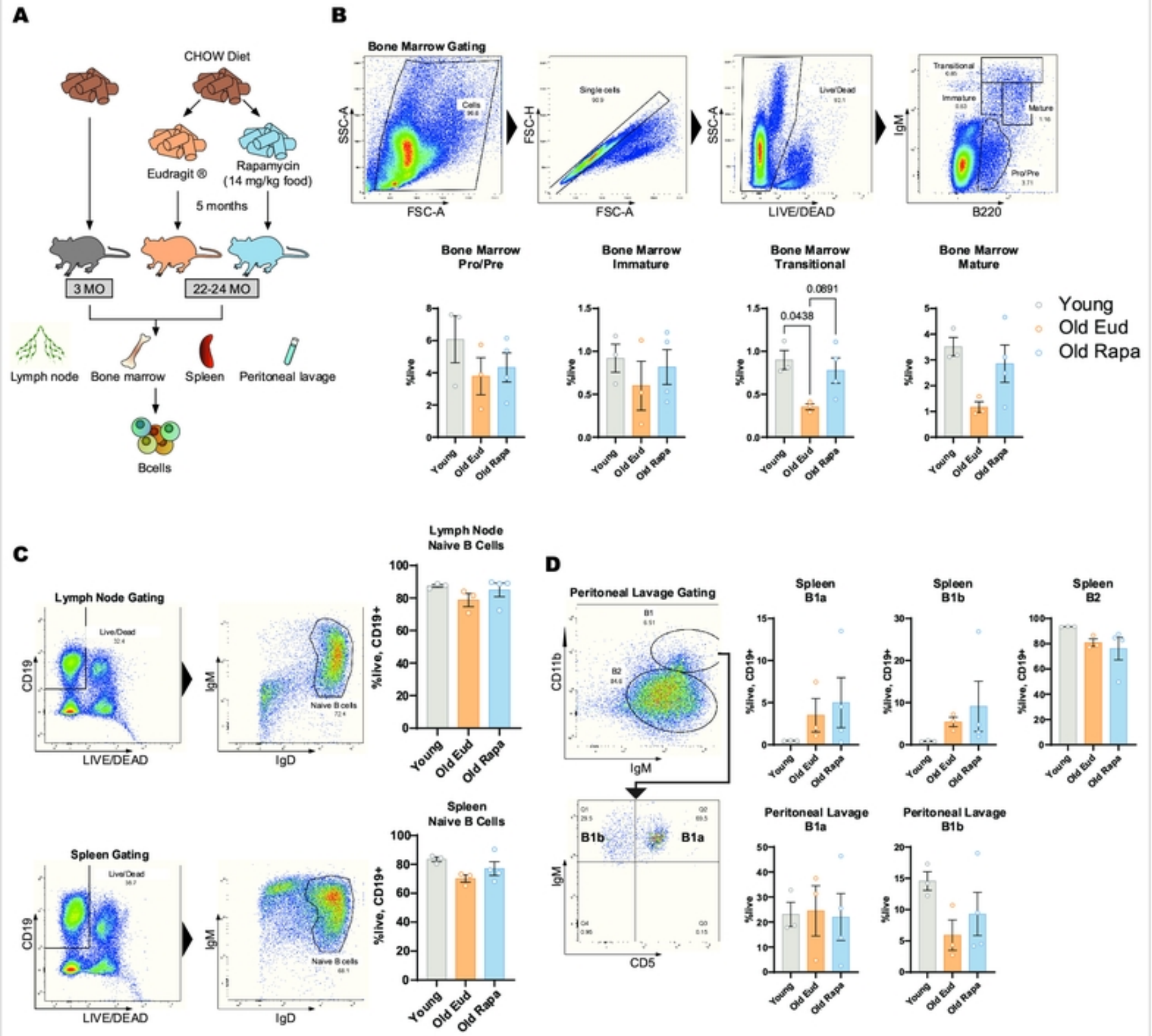

Figure 2

Figure 4, Torrent *et al.*

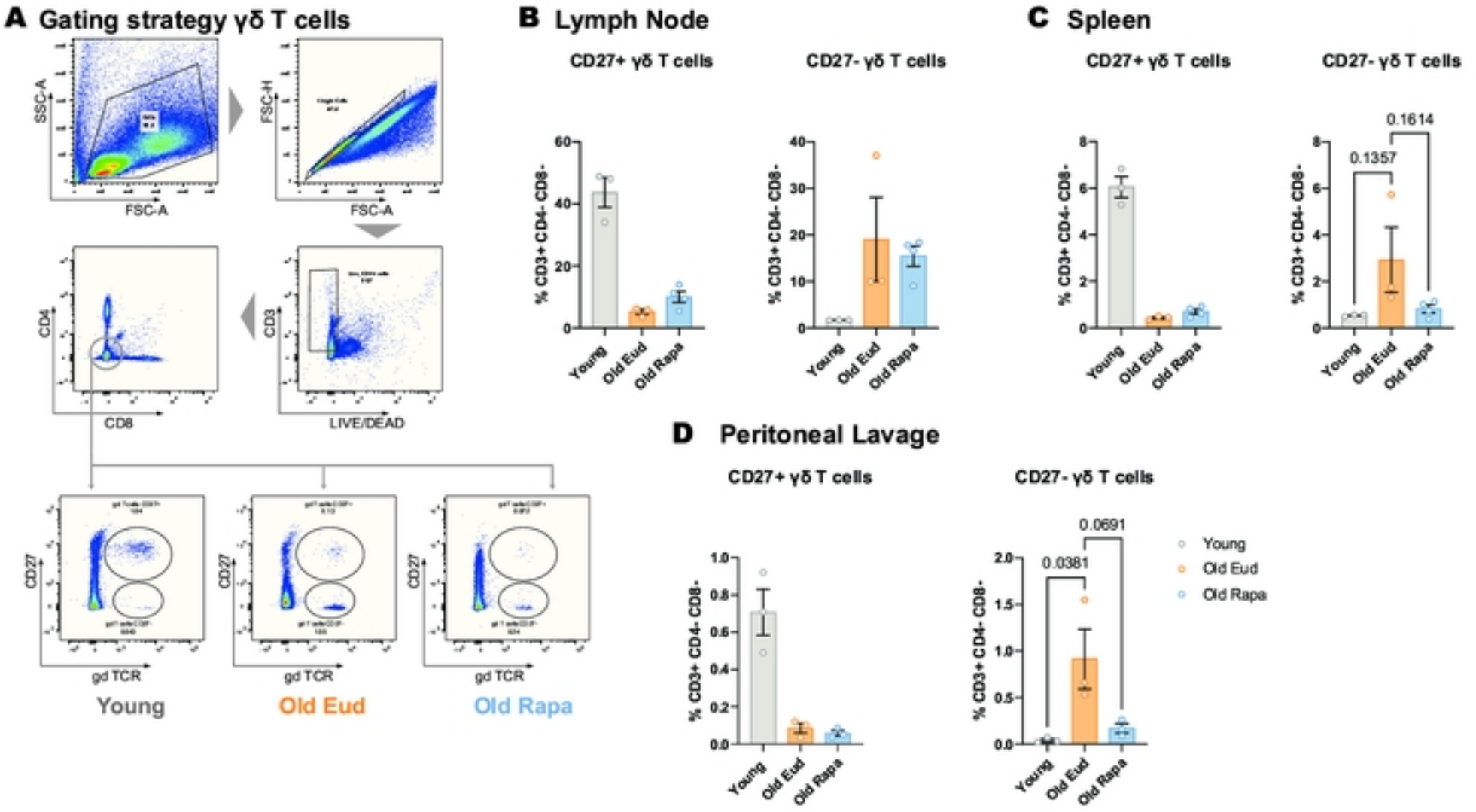

Figure 4